Plasmon Enhanced Fluorescence with Aggregated Shell-Isolated Nanoparticles

ARTICLE *in* ANALYTICAL CHEMISTRY · SEPTEMBER 2014

Impact Factor: 5.64 · Source: PubMed

4 AUTHORS, INCLUDING:

Ariel R Guerrero

University of Chile

17 PUBLICATIONS **197** CITATIONS

SEE PROFILE

Pablo Albella

Imperial College London

53 PUBLICATIONS **786** CITATIONS

SEE PROFILE

Ricardo F Aroca

University of Windsor

314 PUBLICATIONS **6,824** CITATIONS

SEE PROFILE

analytical chemistry

Article

pubs.acs.org/ac

Plasmon Enhanced Fluorescence with Aggregated Shell-Isolated Nanoparticles

Igor O. Osorio-Román,[†,§] Ariel R. Guerrero,[†] Pablo Albella,[‡] and Ricardo F. Aroca*[,†]

[†]Materials and Surface Science Group, Department of Chemistry and Biochemistry, University of Windsor, Windsor, Ontario, Canada, N9B 3P4

[‡]Experimental Solid State Group, Department of Physics, Imperial College London, SW7 2AZ, London, United Kingdom

[§]Departamento de Química Inorgánica, Facultad de Química, Pontificia Universidad Católica de Chile, 7820436, Santiago, Chile

Supporting Information

ABSTRACT: Shell-isolated nanoparticles (SHINs) nanostructures provide a versatile substrate where the localized surface plasmon resonances (LSPRs) are well-defined. For SHINEF, the silver (or gold) metal core is protected by the SiO_2 coating, which is thicker than the critical distance for minimum quenching by the metal. In the present work, it is shown that an increase in the SHINEF enhancement factor may be achieved by inducing SHIN aggregation with electrolytes in solution. The proof of concept is demonstrated using NaCl as aggregating agent, although other inorganic salts will also aggregate SHIN nanoparticles. As much as a 10-fold enhancement in the SHINEF enhancement factor (EF) may be achieved by tuning the electrolyte concentrations in solution. The SHINEF experiments include the study of the aggregation effect controlling gold SHIN's surface concentration via spraying. Au-SHINs are sprayed onto layer-by-layer (LbL) and Langmuir−Blodgett (LB) films, and samples are fabricated using fluorophores with low and also high quantum yield.

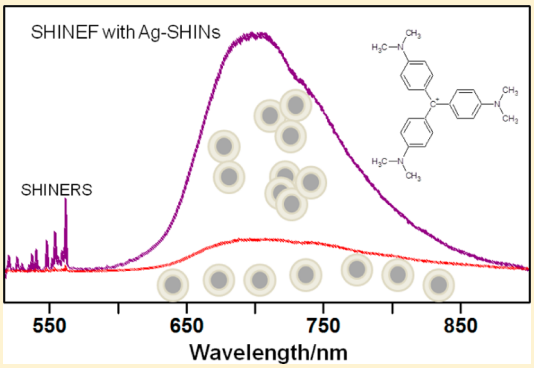

SHINERS[1] and SHINEF[2] are acronyms used for plasmon enhanced scattering and fluorescence observed with shell-isolated nanoparticles (SHINs). For scattering, the coating of the metal core is made as thin as possible (~2 nm). However, for surface enhanced fluorescence (SEF)[3] or metal enhanced fluorescence (MEF),[4] there is a critical fluorophore−metal distance for maximum enhancement.[3,5] When an incident field E_0 impinges on a metallic nanostructure, an enhanced local field E_{loc} is observed.[6] The ratio leads to a local enhancement factor $|E| = |(E_{loc}/E_0)|$. The plasmonic origin of enhancement leads to surface enhanced fluorescence (SEF) proportional to $|E|^2$, and surface enhanced Raman scattering (SERS) proportional to $|E|^4$.[7,8] In a previous report,[9] it was shown that recording SHINERS and SHINEF for a low quantum yield molecule and Ag-SHINs in solution can provide direct experimental evidence for the predicted local enhancement dependence of the measured spectroscopic signal. The latter measurements in solution of molecules adsorbed onto mainly isolated Ag-SHINs were characterized for very modest enhancement factors (EF). In this work, we look at the increase of the EF by aggregating SHIN nanoparticles. The effect of aggregation with Ag and Au colloids is well-known in the literature;[10,11] in particular, interparticle junctions in aggregated nanoparticles serve as hot-spots for field enhancement in nanometric spatial locations.[12] Aggregated nanoparticles are shown experimentally, and when the fluorophore is at the appropriate distance from the surface, efficient SEF is observed, where enhancement factors are in the range of 15−750.[13] Recently, self-assembled aggregates of Ag nanoparticles produced by introducing polyacrylamide into Ag colloids have been shown to enhance fluorescence of a high quantum yield fluorescein isothiocyanate isomer by more than 27-fold.[14] We explore here SHIN's aggregation, first in solution to demonstrate the increase in the EF solely due to the formation of aggregates. Further, we look at the aggregation effect using spraying techniques on layer-by-layer (LbL) and Langmuir−Blodgett (LB) samples of high and low quantum yield molecules. In addition, finite-difference time-domain (FDTD) computations qualitatively illustrate the near field and far field enhancement trend, as SHIN's dimer gap is decreased.

EXPERIMENTAL SECTION

Crystal violet (CV, total dye content 90%) was purchased from Fisher Scientific. Malachite green and Eosin-Y (total dye content 50%), 3-aminopropyltrimethoxysilane (APTMS), and tetraethylorthosilicate (TEOS, 98%) were purchased from Sigma-Aldrich and used as received. Octadecyl Rhodamine B (R18) was obtained from Invitrogen. Unless otherwise specified, solutions are aqueous and the water employed is

Received: July 1, 2014
Accepted: September 16, 2014

   dx.doi.org/10.1021/ac502424g | Anal. Chem. XXXX, XXX, XXX−XXX

Milli-Q quality (18.2 MΩ·cm). All glassware was cleaned using aqua regia and rinsed with abundant Milli-Q water.

Silver-SHINs.[9] The core silver colloids were prepared by reduction of silver nitrate with sodium citrate, similarly to the classical Lee–Meisel method.[15] 18 mg of $AgNO_3$ was dissolved in 100 mL of water, and the solution was brought to a vigorous boil. Then, 2 mL of a 1% w/v sodium citrate aqueous solution was added, and boiling was continued for approximately 1 h. After that, the solution was removed from the heat and 6 mL of a 1 mM solution of 3-aminopropyltriethoxysilane (APTES) was added. The solution stirred for approximately half an hour; subsequently, it was brought to a boil, and 24 mL of activated sodium silicate solution 0.54% w/v was added. The activation is done by bringing the pH of the solution down from its original pH (>11) to 10.5 by adding the beads of an acidifying resin (Amberlite IR-120). The boiling was continued for 3 h. Finally, the resulting SHIN particles were centrifuged at 12 000 rpm for 7 min, to concentrate the particles, reducing 36 mL of the original colloid to two 1.5 mL microcentrifuge tubes. Aliquots of this concentrated dispersion were used for the SHINEF experiments in solution.

Gold-SHINs.[2] 200 mL of 0.01% $HAuCl_4$ (w/v) is brought to boiling in a round-bottom flask equipped to a condenser, with vigorous magnetic stirring in a sand bath. When the solution started to boil, 3.2 mL of 1% (w/v) trisodium citrate was added. A purplish red color started to develop within 1 min; heating and magnetic stirring was continued for another 10 min. The heat was then removed, but the stirring continued for 15 min. A small amount of the resulting colloids was characterized with UV–vis absorption and shows a surface plasmon absorption peak at 520 nm. For gold coating, 6 mL of a freshly prepared solution of 1 mM APTMS is added to 100 mL of the colloidal solution under vigorous magnetic stirring. Meanwhile, a 0.54% (w/v) sodium silicate solution is prepared and activated by adjusting its pH down between 10.2 and 10.3 using the cation exchange resin to prompt the formation of silica. Then, the solution is heated again in a sand bath to 95 °C, and 16 mL of the active sodium silicate solution is added. Coating is continued for 100 min. The resulting SHIN solution is concentrated by centrifugation at 12 000 rpm for 7 min, and the supernatant is discarded.

In addition to SHINEF experiments in solution, two thin film techniques were used to fabricate samples of fluorophores: the layer-by-layer (LbL) technique[16] and the Langmuir–Blodgett method.[17] For LbL samples, the surface of quartz slides is modified with polyelectrolyte MADQUAT 4% (w/v) followed by Eosin-Y. The quartz slides were sonicated, in turn, in acetone, NaOH (1M), 1:1 (v/v) ethanol/water, and water, for about 15 min each. Electrostatic LbL assemblies (MADQUAT/Eosin-Y) were grown by alternately immersing the slides in the polycation solution (+) and the as-obtained Eosin Y solution (−), for about 20 min each. Between each step, the surface was immersed in Milli-Q water for 5 min and dried under a nitrogen stream or under vacuum. The water used for washing was changed between each immersion. To form LbL with crystal violet, we use the same protocol above, but we change the polyelectrolyte to PAA (poly(acrylic acid)); we prepare a solution of PAA 4% to pH = 8.0 in Milli-Q water.

An LB mixed monolayer of R18 and arachidic acid is prepared by spreading 250 μL of (1–100) molecular ratio of R18-AA on a Milli-Q water–air interface; the solution was left for 30 min to ensure complete evaporation of dichloromethane used as the solvent. After solvent evaporation, a set of barriers compressed the floating film to a maximum pressure of 25 mN/m, and pressure is kept constant at this value during transfer to a slide of quartz. We used water as a solvent for nanoparticle spraying. A 2D spatial mapping of a small surface area with and without SHINs is recorded. The spectra without SHINs provide the reference. The statistical study (Figures S4, S5, and S6, Supporting Information) corresponds to set of 100 spectra measured on the surface with SHINs. The enhancement factor is calculated by integration of the band area with and without SHINs.

Fluorescence and SHINEF spectra were recorded using a Renishaw micro-Raman system RM 2000. This system is equipped with a Peltier charge-coupled device (CCD) detector and Leica microscope. Fluorescence spectra were obtained using the 514.5 nm excitation line of an argon-ion laser. Measurements on solids were recorded in backscattering geometry using a 20× microscope objective with a numerical aperture value of 0.40. Measurements on liquid were recorded using a macro objective adapter for measurements in quartz cuvettes. Finally, all spectral acquisition conditions were chosen to avoid sample degradation.

RESULTS AND DISCUSSIONS

Ag-SHINs Aggregation in Solution. Partial aggregation can be induced in a colloidal dispersion by adding electrolytes[11,18] such as NaCl or KCl, and the aggregates may provide hot spots that are associated with the large enhancement factors in SERS. Indeed, this is how Kneipp et al.[19] in 1997 achieved single-molecule detection. Here, an attempt to aggregate SHIN particles and investigate the effect on the EF is described. The CV and MG solution aggregation experiments are carried out using quartz cuvettes. The plasmon absorption of the silver colloids and Ag-SHINs and the extinction spectra of low quantum yield CV and MG molecules are given in Figure 1. A

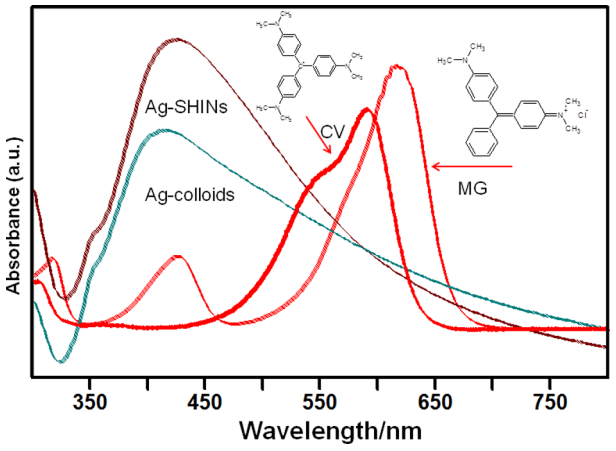

Figure 1. Plasmon absorption of Ag-colloids and Ag-SHINs. UV–vis absorption spectra of CV and MG molecules in solution.

total of 1 mL of solution was always employed, using a fixed quantity of dye. In the case of CV, it was done by adding a fixed aliquot from a CV stock solution, 100 μL of a 6×10^{-5} M solution, and then adding aliquots of concentrated SHINs solution (100 μL). To see the effect of aggregation, we added aliquots of a 0.1 M NaCl solution until the specified concentration (0.01 to 0.08 M) was achieved, added Milli-Q water until reaching 1 mL, and then mixed it all in an Eppendorf tube. (In the last case, with 0.08 M NaCl, it was all

dx.doi.org/10.1021/ac502424g | Anal. Chem. XXXX, XXX, XXX–XXX

NaCl solution and no additional water was added, as it was 100 μL of dyes, 100 μL of particles, and 800 μL of NaCl solution). The results are shown in Figures 2 and 3 for CV and MG, respectively. It can be appreciated that the aggregation effect provides an improvement in the EF of almost an order of magnitude for the CV fluorescence and the MG fluorescence. Similar aggregation measurements for MG, carried out with the 632.8 nm laser line, also show higher SHINEF enhancement factor as shown in Figure S1, Supporting Information. It should be pointed out that the concentration of the fluorophore and that of the SHINs remains constant; the variable concentration is that of the aggregating agent. Therefore, the increase in fluorescence enhancement can be directly attributed to SHIN's aggregation. The aggregating effect of the NaCl electrolyte on the absorption spectrum of CV in solution is also observed, where a decrease in monomer absorption is evident with an increase in electrolyte concentration (from 0.01 to 0.08 M of NaCl) as shown in Figure S2, Supporting Information. The observed change in the plasmonic properties due to aggregation would also lead to spectra profile modification[20] of the observed enhanced fluorescence as could be seen here in Figure 2 and in practically all the SHINEF spectra.

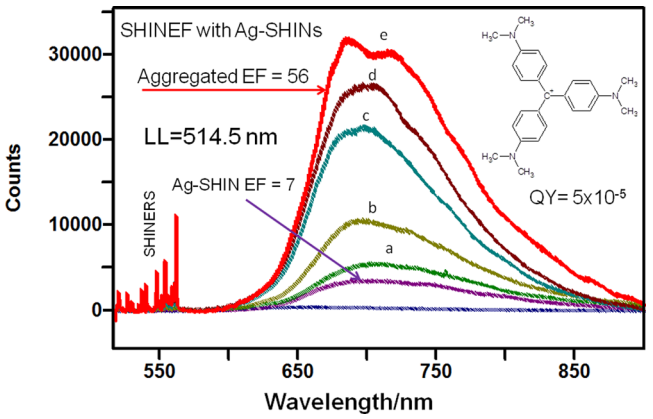

Figure 2. Aggregating effect of the NaCl electrolyte on SHINEF and SHINERS enhancement is illustrated for CV in solution. (a) In NaCl 0.01 M, (b) in NaCl 0.02 M, (c) in NaCl 0.03 M, (d) in NaCl 0.05 M, and (e) in NaCl 0.08 M.

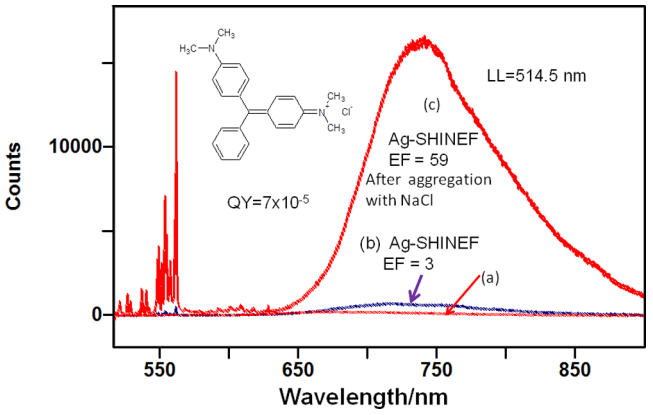

Figure 3. Aggregating effect of the NaCl electrolyte on SHINEF and SHINERS enhancement is illustrated for MG in solution. (a) Reference fluorescence. (b) SHINEF before aggregation. (c) SHINEF after aggregation.

Spraying Au-SHINs Nanoparticles. Au-SHIN nanoparticles were selected for the spraying studies given that Au-SHINs are more resilient than Ag-SHINs and they have a more extended lifetime. We use AirBrish Master Model G44 for deposition of Au-SHIN nanoparticles on the samples. This method provides coverage to the surface with many tiny droplets. Because these droplets are small and cover the whole surface, the nanoparticles will be distributed more evenly and any aggregation due to solvent evaporation will be highly localized within the fine mist droplets. We control some parameters for the Airbrush, sample distance and working pressure; the optimal distance was 30 cm, and the pressure was 43 psi. Also, the thickness of SHIN deposition was measured with a quartz crystal microbalance INFICON Model XTC (See Supporting Information, Figure S3). The plasmon absorption of the Au colloids and Au-SHINs are shown in Figure 4, together with two scanning electron microscopy (SEM) images of selected nanostructures.

Computations of the near field enhancement for isolated Au-SHIN leads to surface enhanced fluorescence proportional to $|E|^2$ and 9-fold enhancement, in agreement with the modest enhancement observed for Au-SHINs in solution.[20] The

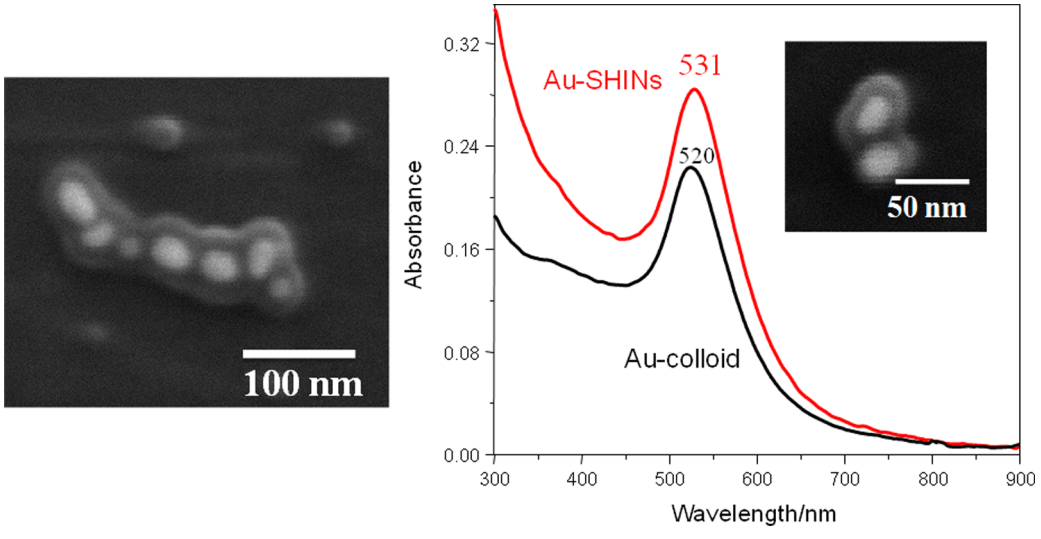

Figure 4. Plasmon absorption and scanning electron microscopy (SEM) images of Au-SHINs.

dx.doi.org/10.1021/ac502424g | Anal. Chem. XXXX, XXX, XXX−XXX

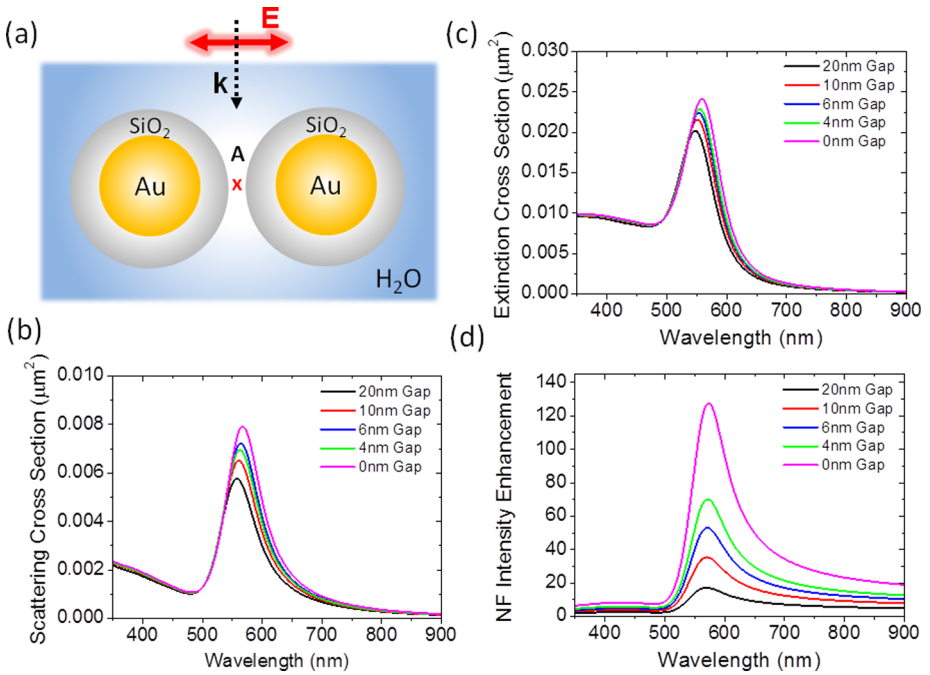

Figure 5. (a) Scattering system composed of a dimer of 2 core−shell nanoparticles, each of them has a 50 nm Au core diameter and 10 nm SiO_2 shell. The dimer is illuminated at normal incidence and polarized along the dimer axis. (b, c) Spectral scattering and extinction cross sections, respectively, for five gap sizes. (d) Near field intensity enhancement in the center of the gap (A point).

simplest model for aggregation is that of the Au-SHIN dimer illuminated at normal incidence and polarized along the dimer axis as shown in Figure 5a. In Figure 5, we show the far field and near field response of a gold SHIN dimer embedded in water. Each SHIN has a 50 nm Au core diameter and 10 nm SiO_2 shell. Figure 5b,c shows the scattering (σ_{sca}) and extinction cross sections (σ_{ext}), respectively, for different gap sizes. The trend is clearly seen, and as the gap is reduced, both the scattering and extinction cross sections magnitudes increase and get spectrally red-shifted. This expected phenomenon is due to the coherent interaction of the plasmonic dipolar resonance excited in both SHINs.[21] This interaction also contributes to the enhancement of the near field intensity in the gap of the dimer, as shown in Figure 5d, where we plot the near field intensity enhancement in the center of the gap. The trend is the same for the metal core of different diameters. The same as in the case of the far field cross sections, the near field response gets enhanced and red-shifted as we make the dimer gap smaller. This effect is in very good agreement with recent experimental and theoretical works showing that the near and far field spectral resonance positions are shifted.[22,23] The results shown in Figure 5d correspond to the NF intensity enhancement, that is always normalized to the incident value (E^2/E_0^2). In order to perform this calculation numerically, it is often assumed that E_0 = 1 V/m.

All these near and far field results have been obtained with a finite-difference time-domain software (Lumerical) using optical data of Palik's reference book.[24] The presented results are fully converged; thus, they can be considered an exact solution of Maxwell's equations. Additionally, some of the results shown here have been tested with other solving methods, COMSOL multiphysics and the discrete dipole approximation (DDA),[25] producing very good agreement. Therefore, plasmonic origin of enhancement by SHIN dimers, with a 50 nm Au core and 10 nm SiO_2 coating, leads to EF of the local field as a function of the inter SHIN distance varying up to a maximum $|E|^2$ EF of 125 (zero gap) or around 60 for a 4 nm gap. Since we are measuring average SHINEF enhancement with a random distribution of aggregates, as can be seen in the SEM inset of Figure 6, it is expected that the observed EF would be lower than the ideal computational model. The best homogeneous sample is the LB mixed monolayer of R18 fluorophore and arachidic acid (1−100) molecular ratio[26] with a fairly high quantum yield. Spraying is carried out in sets of 5, 15, and 30, and after drying the surface, fluorescence spectra were collected with a 20× objective and 514.5 nm excitation. The SHINEF spectra reveal enhancement in all points of the surface covered by spraying 5, 15, or 30 times. However, a histogram of the frequency of finding a given EF in 100 spectra

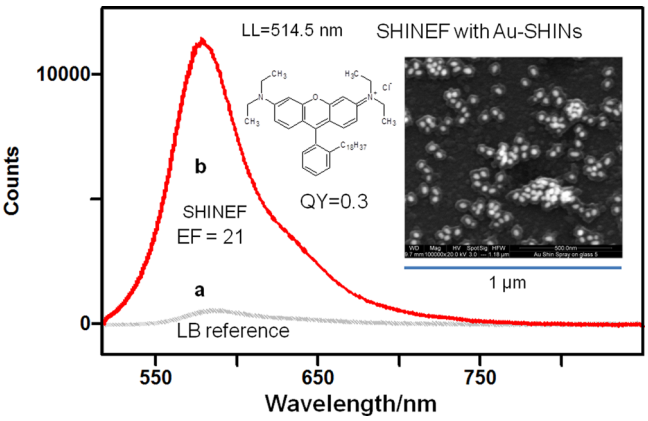

Figure 6. SHINEF from Au-SHINs sprayed onto a monolayer LB film containing the R18 chromophore mixed with arachidic acid (1:100). (a) Reference LB fluorescence. (b) SHINEF spectrum of R18 corresponding to the maximum EF value of 21-fold with 5 sprays. Inset shows the SEM image at a random location on the surface formed with 5 sprays of SHINs.

dx.doi.org/10.1021/ac502424g | Anal. Chem. XXXX, XXX, XXX−XXX

indicates a fairly random distribution of EF in the 5 spray (shown in Figure S3, Supporting Information) and a maximum EF of 21, which is higher than the EF calculated for an isolated Au-SHIN. Variable EFs are observed in all three spraying conditions. Notably, in the case of the R18 sample, at 30 sprays, there is saturation, probably due to clumping and reabsorption, and the maximum recurrent EF is lower than those seen in the 5 or 15 spray experiments. Similar results were found for the high quantum yield Eosin-Y sample prepared using the LbL technique and given in Figure 7 (and Figure S5, Supporting

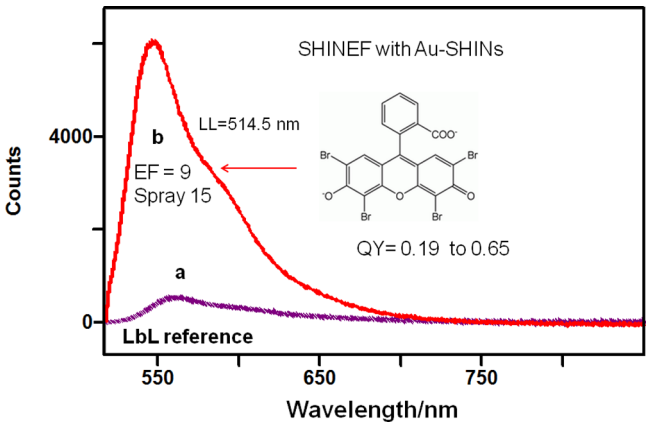

Figure 7. SHINEF of high quantum yield Eosin-Y from Au-SHINs sprayed onto an LbL film containing the chromophore. (a) LbL reference fluorescence. (b) For the Eosin-Y fluorophore, the maximum EF value is 9-fold.

Information). Again, Eosin-Y is a molecule with a high quantum yield (QY = 0.65 in ethanol,[27] 0.32[28] and 0.19 in water solution). The maximum EF obtained with aggregation is a 9-fold enhancement, in the same range with the EF (4.3) recently reported on a plasmonic nanostructure.[28] It should be pointed out that the chromophore surface concentration in the LB monolayer is more homogeneous and lower (it is a mixed film) than the chromophore concentration in the LbL samples. Finally, using the LbL technique, a layer of crystal violet (very low quantum yield) was prepared electrostatically onto poly(acrylic acid). The results are illustrated in Figure 8. A

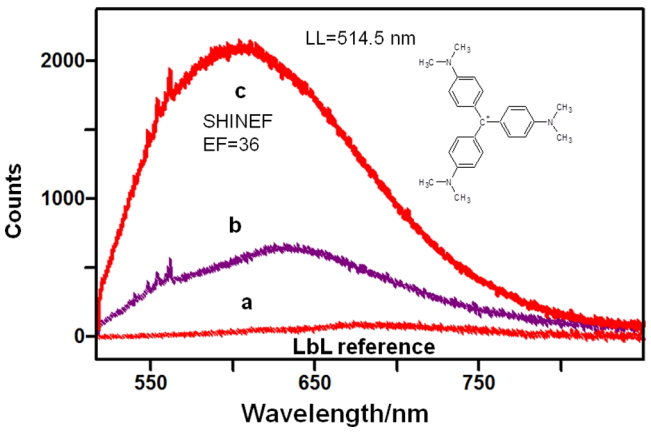

Figure 8. SHINEF of a low quantum yield CV LbL film. (a) LbL reference fluorescence. (b) Typical SHINERS and SHINEF spectra recorded on the LbL CV film with 15 sprays. (c) For this sample, the maximum EF value is 36-fold with 30 sprays.

high EF of ~36 was observed with strong aggregation (15 and 30 sprays shown in Figure S6, Supporting Information). Since the quantum efficiency is very low, the SHINERS spectra can also be seen, helping with the vibrational identification of the CV adsorbate.

The fact that SHINEF is observed for both high and low quantum yield molecules is significant. Some reports show a tendency to dismiss the SEF or MEF effect for high quantum yield chromophores: "*The enhancement effect is most significant for relatively weak and diluted absorbers and rather inefficient emitters that are placed in close proximity to the metal nanoparticles.*"[29] The experimental results show that high QY fluorophores can also provide large fluorescence EFs. For instance, Gartia et al.[28] measured an EF of 20.5 for R6G (QY = 0.9) and an EF of 100 for fluorescein (QY = 0.95). In summary, practitioners should not be discouraged to try high quantum yield molecules in SEF, MEF, or SHINEF applications.

CONCLUSIONS

An increase in the SHINEF enhancement factor is demonstrated by inducing SHIN aggregation with NaCl in solution. As much as a 10-fold enhancement in the EF may be achieved by tuning the electrolyte concentrations. The results are supported by computations of local field enhancement of Au-SHIN's dimers. Therefore, the improvements are assigned to contributions of high local field enhancement in small SHIN aggregates. Experiments with LB monolayers and LbL samples result in enhancement for high and low quantum yield molecules.

ASSOCIATED CONTENT

Supporting Information

Additional information as noted in text. This material is available free of charge via the Internet at http://pubs.acs.org/.

AUTHOR INFORMATION

Corresponding Author

*E-mail: raroca1@cogeco.ca.

Notes

The authors declare no competing financial interest.

ACKNOWLEDGMENTS

Funding from the National Science and Engineering Research Council of Canada (NSERC) is gratefully acknowledged.

REFERENCES

(1) Li, J. F.; Huang, Y. F.; Ding, Y.; Yang, Z. L.; Li, S. B.; Zhou, X. S.; Fan, F. R.; Zhang, W.; Zhou, Z. Y.; Wu, D. Y.; Ren, B.; Wang, Z. L.; Tian, Z. Q. *Nature* **2010**, *464*, 392−395.

(2) Guerrero, A. R.; Aroca, R. F. *Angew. Chem., Int. Ed. Engl.* **2011**, *50*, 665−668.

(3) Wokaun, A.; Lutz, H. P.; King, A. P.; Wild, U. P.; Ernst, R. R. *J. Chem. Phys.* **1983**, *79*, 509−514.

(4) Geddes, C. D.; Lakowicz, J. R. *J. Fluoresc.* **2002**, *12*, 121−129.

(5) Anger, P.; Bharadwaj, P.; Novotny, L. *Phys. Rev. Lett.* **2006**, *96*, 113002−113004.

(6) Maier, S. A. *Plasmonics: Fundamentals and Applications*; Springer: New York, 2007.

(7) Moskovits, M. *Rev. Mod. Phys.* **1985**, *57*, 783−826.

(8) Le Ru, E. C.; Etchegoin, P. G. *Chem. Phys. Lett.* **2006**, *423*, 63−66.

(9) Guerrero, A. R.; Zhang, Y.; Aroca, R. F. *Small* **2012**, *8*, 2964−2967.

(10) Kneipp, K.; Kneipp, H.; Itzkan, I.; Dasari, R. R.; Feld, M. S. *Chem. Rev. (Washington, D. C.)* **1999**, *99*, 2957−2975.
(11) Kruszewski, S.; Cyrankiewicz, M. *Acta Phys. Polym., A* **2012**, *121*, A68−A74.
(12) Kleinman, S. L.; Frontiera, R. R.; Henry, A.-I.; Dieringer, J. A.; Van Duyne, R. P. *Phys. Chem. Chem. Phys.* **2013**, *15*, 21−36.
(13) Gill, R.; Le Ru, E. C. *Phys. Chem. Chem. Phys.* **2011**, *13*, 16366−16372.
(14) Xia, B. H.; He, F.; Li, L. D. *Colloids Surf., A* **2014**, *444*, 9−14.
(15) Lee, P. C.; Meisel, D. *J. Phys. Chem.* **1982**, *86*, 3391−3395.
(16) Decher, G. *Science* **1997**, *277*, 1232−1237.
(17) Roberts, G. *Langmuir-Blodgett Films*; Plenum Press: New York, 1990.
(18) Garcia-Ramos, J. V.; Sanchez-Cortes, S. *J. Mol. Struct.* **1997**, *405*, 13−28.
(19) Kneipp, K.; Wang, Y.; Kneip, H.; Perelman, L. T.; Itzkan, I.; Dasari, R. R.; Feld, M. *Phys. Rev. Lett.* **1997**, *78*, 1667−1670.
(20) Aroca, R. F.; Teo, G. Y.; Mohan, H.; Guerrero, A. R.; Albella, P.; Moreno, F. *J. Phys. Chem. C* **2011**, *115*, 20419−20424.
(21) Weber, D.; Albella, P.; Alonso-Gonzalez, P.; Neubrech, F.; Gui, H.; Nagao, T.; Hillenbrand, R.; Aizpurua, J.; Pucci, A. *Opt. Express* **2011**, *19*, 15047−15061.
(22) Alonso-Gonzalez, P.; Albella, P.; Neubrech, F.; Huck, C.; Chen, J.; Golmar, F.; Casanova, F.; Hueso, L. E.; Pucci, A.; Aizpurua, J.; Hillenbrand, R. *Phys. Rev. Lett.* **2013**, 110.
(23) Moreno, F.; Albella, P.; Nieto-Vesperinas, M. *Langmuir* **2013**, *29*, 6715−6721.
(24) Palik, E. D. In *Handbook of Optical Constants of Solids*, Palik, E. D., Ed.; Academic Press: San Diego, 1997.
(25) de la Osa, R. A.; Albella, P.; Saiz, J. M.; Gonzalez, F.; Moreno, F. *Opt. Express* **2010**, *18*, 23865−23871.
(26) Goulet, P. J. G.; Aroca, R. F. *Anal. Chem. (Washington, DC, United States)* **2007**, *79*, 2728−2734.
(27) Lakowicz, J. R. *Principles of Fluorescence Spectroscopy*, 3rd ed.; Springer: New York, 2006; Vol. *1*, p 954.
(28) Gartia, M. R.; Eichorst, J. P.; Clegg, R. M.; Liu, G. L. *Appl. Phys. Lett.* **2012**, *101*, 023118.
(29) Sun, G.; Khurgin, J. B. *IEEE J. Sel. Top. Quantum Electron.* **2011**, *17*, 110−118.